An Omni-Directional Static Pressure Probe

RICHARD W. MIKSAD

Department of Civil Engineering, The University of Texas at Austin

(Manuscript received 18 August 1975, in revised form 4 October 1976)

ABSTRACT

A rugged field experiment version of the double-disk static pressure probe is described. The probe consists of two circular disks placed one over the other. Static pressure is sensed through two mutually facing sensing ports located in the center of each disk. Static pressure errors induced by air flow curvature over the leading edges of the disks are minimized through the introduction of shallow dimples centered about the sensing ports. Optimal angle-of-attack performance is obtained by varying the spacing between the disks. Wind tunnel tests were performed to determine the respective influence of disk thickness, dimple geometry and disk separation distance on the response of the probe to vertical and horizontal variations in wind direction and speed. The results show that the introduction of sensing port dimples on reasonably thick plate probes can reduce curvature-induced errors to less than 1% of the dynamic velocity head, and that angle-of-attack errors can be kept to $\pm 0.5\%$ over $\pm 14°$ variations in wind direction.

1. Introduction

The accurate measurement of static pressure under conditions of varying mean wind speed and direction poses a significant problem. Numerous attempts have been made to mount basically uni-directional probes on rotating and sometimes gimballed wind-vane-following mechanisms. However, the fragile nature of these vane arrangements somewhat limit their usefulness in the field. Robertson (1972) reported on a double-disk static probe which had no moving parts and which was fairly insensitive to horizontal and vertical variations in wind direction. Robertson's probe was fairly large (30 cm in diameter) and not as rugged as one would like for field use.

As part of an attempt to measure surface geostrophic winds during the 1972 JONSWAP field experiment (Hasselmann, 1973), we tried to develop a more rugged but accurate version of the double-disk probe. As Thompson (1975) notes, an accuracy of roughly 0.1 mb in measured pressure difference between ships or field stations 200 km apart is required to give a wind accuracy of 0.35 m s^{-1} (and direction to 2°) for a typical wind speed of 10 m s^{-1}. Thus, one needs to reduce measurement errors as much as possible (both on an absolute basis for each probe and on a relative basis between probes) to obtain reasonably accurate data under the variable wind speed and angle-of-attack conditions encountered in field experiments.

This paper reports on a reduced scale, more rugged version of the double-disk design which utilizes shallow dimples to minimize static pressure errors induced by air flow curvature over the probe. Elliott (1972) used a similar compensating dimple technique in a single-disk pressure probe, and several other variations can be found in Bryer and Pankhurst (1971). The probes described here are suited for isolated field station work. Preliminary versions were successfully used over a continuous three-week period during the 1972 JONSWAP project.

2. Probe description

The basic probe (see Fig. 1) consists of two disks, located one over the other, with mutually facing sensing ports. The disks are separated by three small-diameter (0.24 cm) spacing rods. Circular symmetry eliminates probe sensitivity to horizontal variations in wind direction. Careful attention was paid to the drilling of the sensing port holes. The sensing holes in a comparison test probe similar to Robertson's were drilled into brass plugs pressed into an aluminum plate, and machined flush with the plate surface. The hole sizes fall in the middle range tested by Franklin and Wallace (1970), who carefully analyzed static pressure errors induced by improper drilling. The sensing ports in the thicker plexiglass test probes with dimples were drilled directly into the plexiglass surface and carefully lapped and polished to remove burrs. However, the polishing process produced slightly rounded hole corners which as reported by Franklin and Wallace can contribute measurement errors. The effects of sensing hole irregularities was not studied. In the test models described in this paper, the two sensing ports were interconnected via external tubing to a balancing T-connector. The balanced pressure signal was then led to a pressure transducer for measurement.

For actual field application, all external tubing was

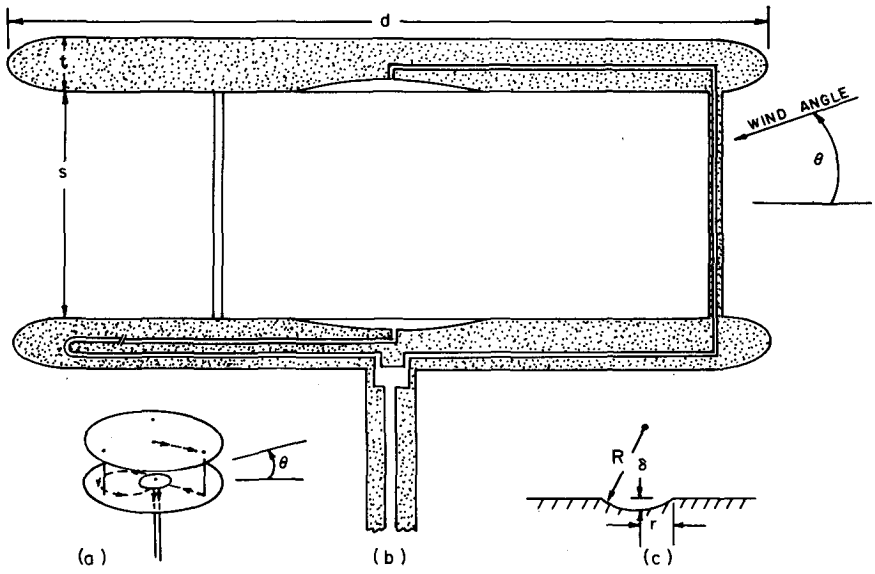

FIG. 1. Schematic drawing (a) of double-disk static pressure probe, with dotted lines indicating path of pressure port routing tubes; (b) cross-sectional detail of field probe (test probe connections to pressure port tubes were made at the right-hand side of each plate and brought to an external connecting T-junction); (c) dimple geometry.

removed and an entirely internal tubing system was devised. The field version is shown in Fig. 1. A channel was milled in the upper side of the top disk and a segment of 0.24 cm brass tubing was potted so as to connect the upper sensing port with a hollow spacing rod. This hollow spacing rod connected to another potted brass tube in the underside of the bottom disk which led to a 1 cm³ balancing plenum chamber in the neck of the mounting support rod. The sensing port on the bottom disk was connected to the plenum chamber by a second channel milled in a circular path so as to have the same path length (i.e., 25 cm) to the plenum chamber as the upper port (Fig. 1a). The averaged pressure signal in the plenum chamber then travelled through a $\frac{3}{8}$ inch tubular support mount via a quick connect coupling to the pressure transducer. This self-contained arrangement was easily machined, and presented virtually no maintenance problems except for the ever-present problem of sensing port contamination by moisture.

3. Probe design

The primary problem, incurred when plate thickness was increased to improve structural ruggedness, was an accompanying increase in static pressure error due to air flow curvature. For a reasonably aerodynamically shaped leading edge, air flow curvature will be minimized as the thickness ratio (i.e., the ratio of plate thickness to plate diameter, t/d) is decreased. In the limit of very small thickness ratio, curvature-induced pressure errors are accordingly small, and $t/d \ll 1$ performance is the standard to which other probes should aspire. Unfortunately, probes with small thickness

TABLE 1. Characteristic dimensions of the five test probes with Robertson's (1972) probe included for comparison.

Probe	Dimple geometry	Disk diameter d (cm)	Thickness ratio t/d	Dimple ratio δ/r	Sensing port diameter (cm)	Spacing post diameter (cm)	Material
Robertson's (1972) probe		30	0.005	0	0.150	0.30	Aluminum sheet
Thin disk comparison probe		15.2	0.011	0	0.109	0.285	Aluminum sheet
Thick disk no dimple		15.2	0.037	0	0.140	0.236	Plexiglass
Thick disk with arc dimple		15.2	0.037	0.02	0.140	0.236	Plexiglass
Thick disk, small, with arc dimple		10.8	0.064	0.025	0.140	0.236	Plexiglass
Thick disk with conical dimple		15.2	0.037	0.02	0.140	0.236	Plexiglass

ratios (i.e., Robertson's $t/d \approx 0.005$, for example) tend to be fragile, and difficult to keep in parallel alignment because of warping of the thin sheet metal disks. For performance evaluation purposes, a comparison probe similar to that of Robertson's with a fairly small thickness ratio of $t/d = 0.011$ (and no dimples) was constructed from aluminum sheet and used as a standard against which our thicker t/d ratio probes could be compared.

The basic probe design parameters used in the test probes were the sensing port hole diameter, the thickness ratio t/d of plate thickness t to plate diameter d, the spacing ratio s/d of plate spacing s to plate diameter d, the ratio δ/r of dimple depth δ to dimple half-width r, and the radius of curvature R_c of the dimples. The edges of the disks were machined to give a smooth, roughly elliptic leading edge. The basic dimensions of the various probes tested are given in Table 1.

No particular theory exists to model the complicated flow and pressure field between a pair of circular plates with mutually facing dimples at an arbitrary angle of attack. However, some useful estimates of probe geometry at zero angle of attack were obtained by treating the centerline flow over the leading edge of a single disk as being similar to that produced by a semi-infinite plane body in a uniform stream (Milne-Thomson, 1960, p. 202), and the subsequent flow over the dimple as similar to that obtained from Milne-Thomson's (p. 172) analysis of the "flow over a ditch." The composite flow was then used to determine the variation in pressure coefficient $C = (p - p_\infty)(\frac{1}{2}\rho U_\infty^2)^{-1}$ over the surface of a dimpled disk. This of course is an ad hoc procedure and must be treated as such. It is outlined below.

If one assumes that q_ϵ (see Fig. 2) the flow speed along the plate at x_ϵ (a point just before the edge of the dimple) can be estimated from the source in a uniform stream solution, and can then be used as the incoming velocity in the flow over a ditch solution, then the pressure coefficient C at the sensing port can be approximated by

$$C(x_p) = 1 - \left\{ \frac{16}{n^4} \left(\frac{1-\cos\xi}{1-\cos 2\xi/n} \right)^2 \frac{h^2}{\pi^2} \times \left[\left(\frac{\pi}{h} + \frac{x_\epsilon}{x_\epsilon^2 + y_\epsilon^2} \right)^2 + \left(\frac{y_\epsilon}{x_\epsilon^2 + y_\epsilon^2} \right)^2 \right] \right\},$$

where $h = t/2$ is the half-thickness of the plate, $\xi = 2\pi/n$, and n is a parameter which specifies the geometry of the dimple in coaxial coordinates. The value of n can be obtained as a solution of the relation

$$-\delta/r = \sin\tfrac{1}{2}n\pi/(1-\cos\tfrac{1}{2}n\pi),$$

where r is the half-width of the dimple and δ the dimple depth at the sensing port. The radius of curvature of the dimple is given by $R_c = r \csc n\pi/2$.

The procedure used here was to specify (r,δ) and hence R_c, for a shallow but machinable dimple.[1] The

[1] The machinability constraint is important, as the radius of curvative (i.e., the radius of lathe cutting tool swing) is of order 65 cm for the shallow dimple used in the $t/d = 0.037$ probe.

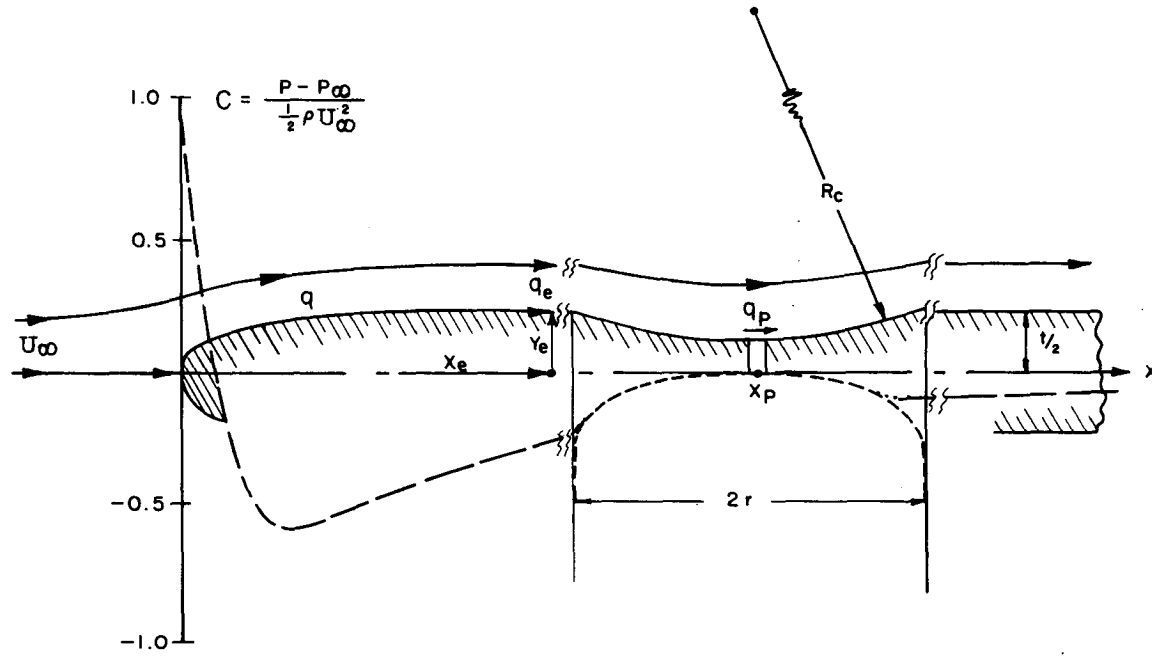

FIG. 2. Schematic diagram of the ad hoc design procedure for pressure error corrections due to air flow curvatures over probe nose and dimple (Milne-Thomson, 1960). Static pressure sensing port is 13.5 plate thickness units behind leading edge of probe in the $t/d = 0.037$ probe. $C = (p - p_\infty)/(\frac{1}{2}\rho U_\infty^2)$, where q is the flow speed along surface stream line and U_∞ the incoming wind speed.

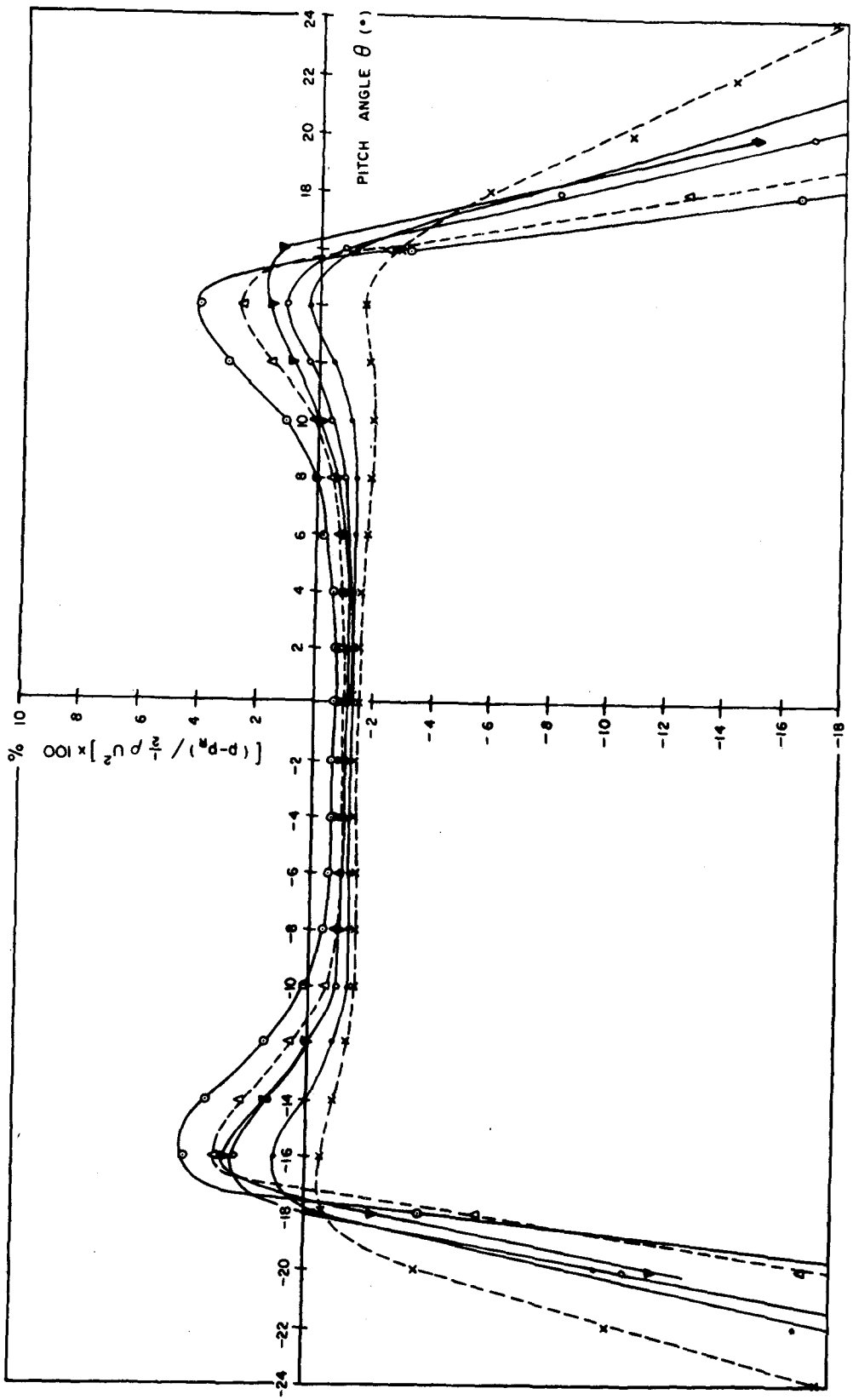

FIG. 3. Percentage static pressure errors (relative to dynamic head $\frac{1}{2}\rho U_\infty^2$) versus disk spacing and pitch angle for the comparison, $t/d=0.011$, thin-disk probe with no compensating sensing port dimples: ⊙, $s/d=0.7$; △, $s/d=0.60$; ▼, $s/d=0.53$; ○, $s/d=0.5$; ●, $s/d=0.47$; ×, $s/d=0.40$.

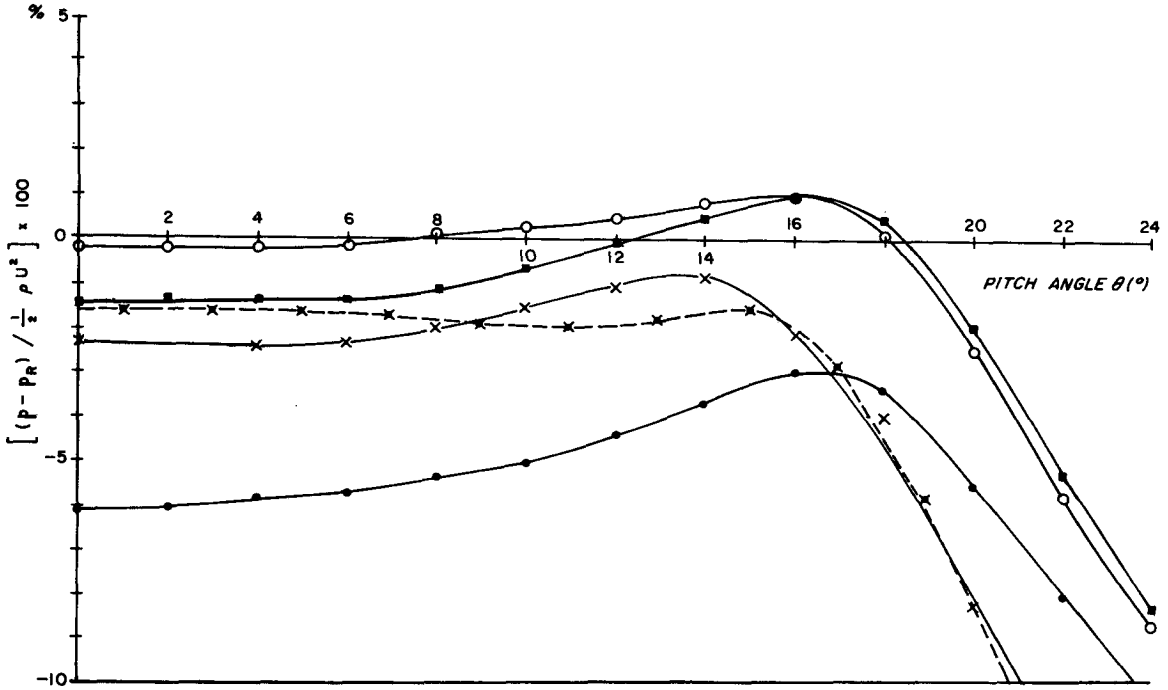

FIG. 4. Comparison of static pressure error characteristics of various t/d ratio probes; disk spacing ratio $s/d=0.4$ for all probes; $U_\infty=10$ m s^{-1}: ×, $t/d=0.011$, no dimples; ●, $t/d=0.037$, no dimples; ○, $t/d=0.037$, spherical dimples; ×, $t/d=0.064$, spherical dimples; ■, $t/d=0.037$, conical shaped dimples.

appropriate value of n was determined and an iterative procedure was used to compute (x_ϵ,y_ϵ) and hence the overall dimensions of the disk such that $C(x_p)\approx 0$ at the sensing port.

Trial-and-error testing and machining showed that this ad hoc procedure gave reasonable starting dimensions for an operational probe. However, it must be stressed that undue reliance should not be placed on the exact dimensions obtained since the actual flow around the probe is highly three-dimensional; has a finite circulation (i.e., lift); is prone to separation; and the flow pattern about each plate and dimple is influenced by the presence of the other mutually facing plate and dimple. In short, the simple two-dimensional potential flow analysis outlined above should only be used for *initial* design estimates.

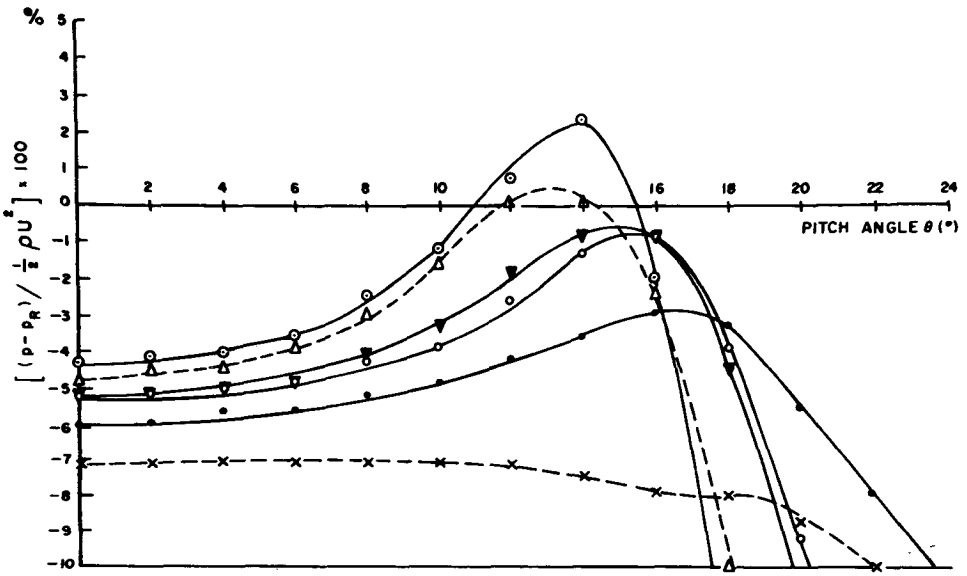

FIG. 5. Details of static pressure error characteristics of a $t/d=0.037$ probe (with no dimples) versus disk spacing and pitch angle for $U_\infty=10$ m s^{-1}: ⊙, $s/d=0.7$; △, $s/d=0.6$; ▼, $s/d=0.5$; ○, $s/d=0.47$; ●, $s/d=0.4$; ×, $s/d=0.3$.

4. Test results

Both the reference and thick-disk probes were tested in the NASA Wind Meter Calibration Tunnel located at the Bay St. Louis-Mississippi Test Facility. The tunnel test section is 1.2 m long, and has a 91 cm diameter circular cross section. Downstream pressure drop over the test section length is 0.15% of the dynamic pressure head. The turbulence level in the test section is less than 0.25%. Errors in measured static pressures were determined by referencing the probe signal to a standard NPL type pitot-static pressure probe placed adjacent to the test probe. An M. K. S. Baratron Model 144 differential capacitive pressure transducer system was used to measure probe errors. The NPL reference static pressure probe signal was fed to one side of the differential transducer head. The test

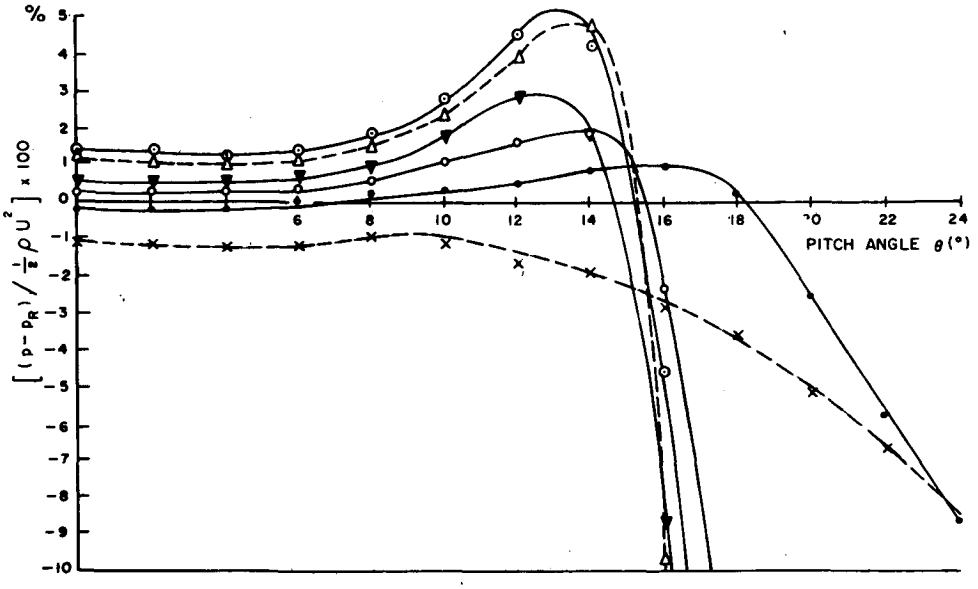

(a)

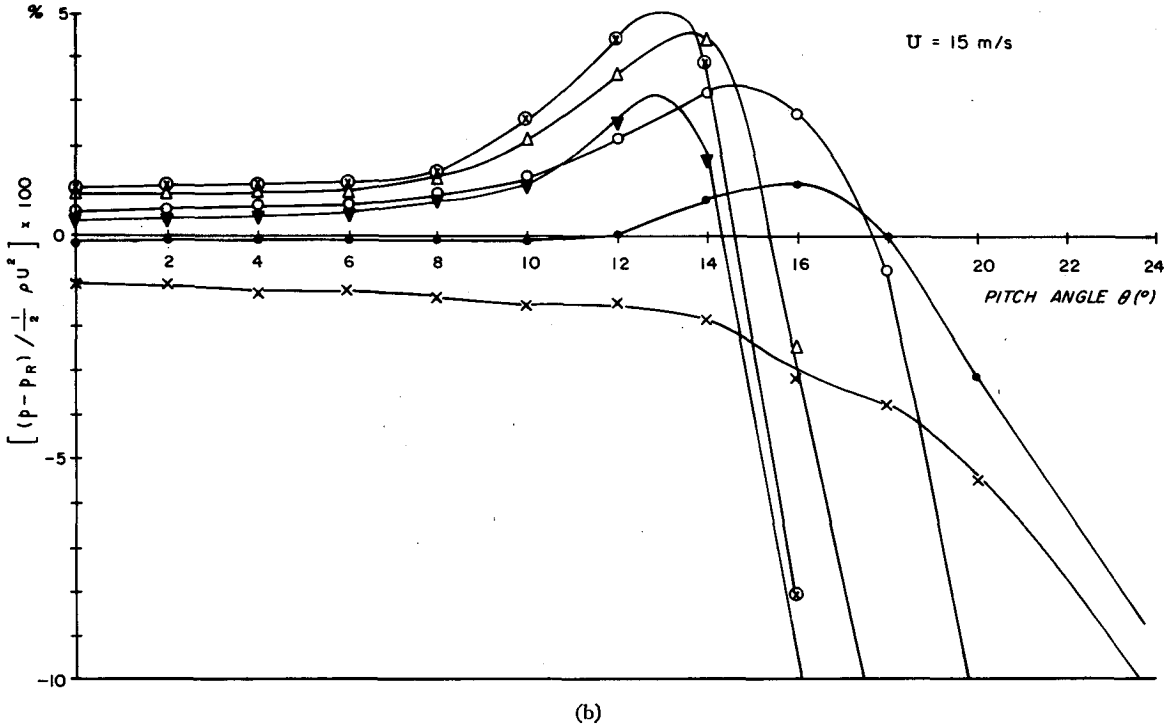

(b)

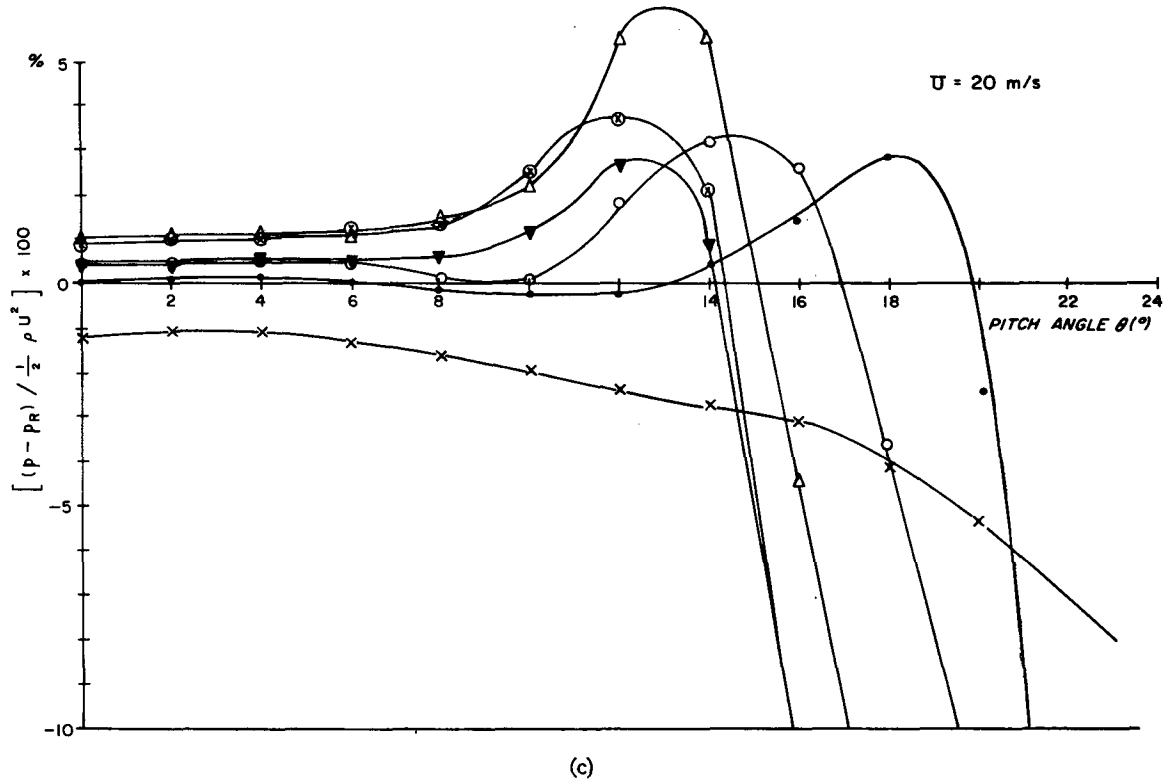

FIG. 6. Details of static pressure error characteristics of a $t/d=0.037$ probe (with spherical dimples) versus disk spacing and pitch angle. (a) $U_\infty=10$ m s^{-1}; (b) $U_\infty=15$ m s^{-1}; (c) $U_\infty=20$ m s^{-1}. ⊙, $s/d=0.8$; △, $s/d=0.7$; ▼, $s/d=0.6$; ○, $s/d=0.5$; ●, $s/d=0.4$; ×, $s/d=0.3$.

probe signal was fed to the other side. The signed, pressure difference signal was then used to determine test probe error. Probes were tested at wind speeds of 10 m s^{-1}, 15 m s^{-1} and 20 m s^{-1}. The error values cited in this section are for 10 m s^{-1} unless otherwise stated. A summary of performance over the 10–20 m s^{-1} range is given in Table 2 for the two best probe designs.

a. Thin, double disk comparison probe (no dimple), $U_\infty=10$ m s^{-1}

As shown in Fig. 3 the sensitivity of the $t/d=0.011$ comparison probe to variations in θ, the vertical angle of wind direction, depends on the plate spacing ratio. The best (i.e., flattest) angle-of-attack response was obtained with a spacing ratio near $s/d=0.4$ or slightly less. As can be seen in Fig. 3, the error curve for $s/d=0.4$ is relatively flat with variations of less than $\pm 0.5\%$ for $\theta=\pm 16°$ variations in vertical wind direction. For spacing ratios significantly smaller than $s/d=0.4$, the error curved tended to bow downward. Although angle-of-attack performance clearly deteriorates as spacing ratio increased or decreased from $s/d\approx 0.4$, $\theta=0$ probe accuracy was found to improve as the spacing ratio was increased. In general, the optimum s/d spacing depends on whether one is most interested in $\theta=0$ accuracy, or in $|\theta|>0$ angle of attack response. For example, while the accuracy of this comparison double-disk probe response for $\theta=0$ (referenced via a differential manometer to an NPL static pressure probe) improved from -1.9% of the dynamic pressure head at $s/d=0.4$, to -0.3% at $s/d=0.7$, the flatness of the angle-of-attack response of the probe deteriorated as s/d increased. All factors considered, the best overall performance for our comparison probe was obtained near $s/d=0.40$.

b. Thick, double disk probes, $U_\infty=10$ m s^{-1}

Both the absolute accuracy and angle of attack performance of our flat surface probes deteriorated as the thickness ratio t/d of the disks was increased to 0.037 or greater (see Fig. 4). However, as noted in Fig. 4, this deterioration could be partially reversed by the introduction of shallow dimples centered at the probe sensing ports. For example, the $\theta=0$ accuracy of the $t/d=0.037$ probe with spherical arc shaped dimples is -0.2% at $s/d=0.4$. In contrast, the $\theta=0$ accuracy of the same $t/d=0.037$ probe with no dimples was -5.9% at $s/d=0.4$. The basic dimple configuration for each probe was determined via testing and the design procedure outlined previously. For a probe with $t/d=0.037$, the most satisfactory dimple was found to have a depth (below the plate surface) of $\delta=0.091t$ at the sensing port, and a radius of curvature of $R=4.2d$. See Table 1 for additional details.

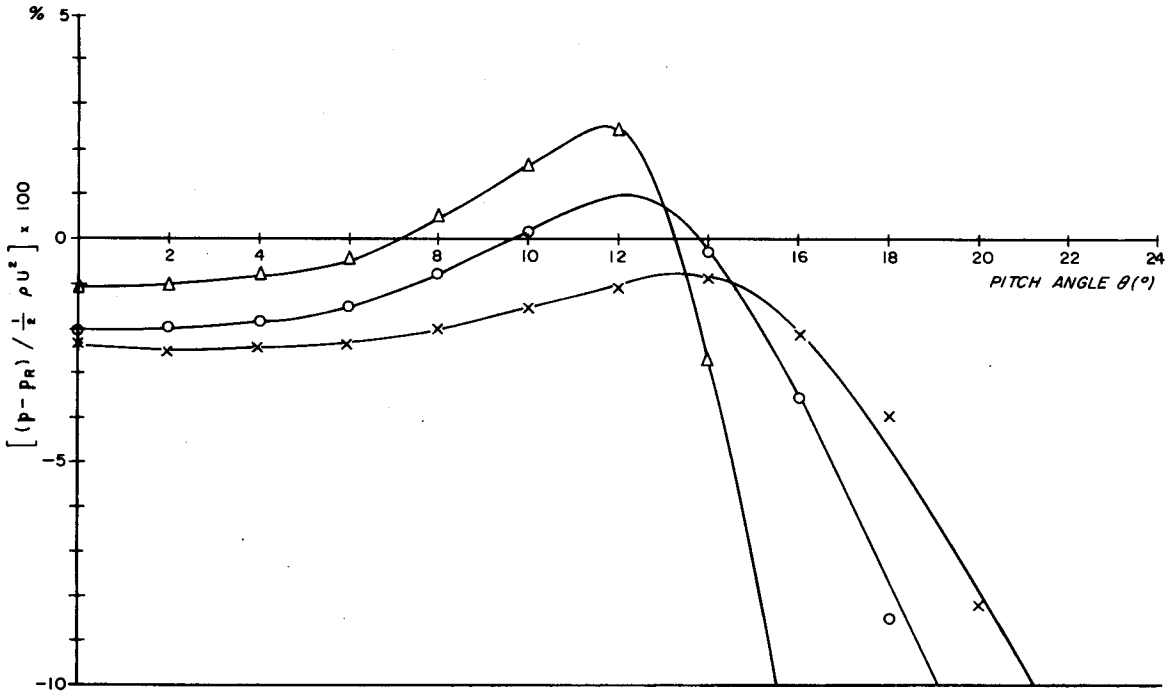

FIG. 7. Details of static pressure error characteristics of a $t/d=0.064$ probe (with spherical dimples) versus disk spacing and pitch angle for $U_\infty=10$ m s^{-1}; △, $s/d=0.57$; ○, $s/d=0.47$; ×, $s/d=0.37$.

Detailed performance characteristics of five different $t/d\geqslant 0.011$ probes are presented in Figs. 4–8 for comparison. Fig. 5 indicates that a thick-disk probe without a compensating dimple has a much poorer $\theta=0$ performance, and a somewhat poorer angle of attack response than the reference $t/d=0.011$ thin-disk probe. However, it can be seen from Fig. 6 that the introduction of a dimple not only served to improve $\theta=0$ accuracy, but also seemed to improve the flatness of the angle-of-attack response relative to that found for the same t/d probe with no dimple. In general, for the $t/d=0.037$ probe, at a spacing ratio near 0.3–0.4, the introduction of a compensating dimple could reduce $\theta=0$ errors to small levels, and at the same time improve angle-of-attack performance to roughly $\pm 0.5\%$ error deviation over a $\theta=\pm 15°$ angle of attack variation.

A compensating arc shaped dimple was also tried in a smaller diameter, $t/d=0.064$ probe to determine whether a thicker t/d probe could still maintain reasonable $\theta=0$ and angle of attack accuracy. This $t/d=0.064$ probe had a disk diameter of 10 cm. (Robertson's $t/d=0.005$ probe, in comparison had a diameter of 30 cm). The results for a 10 m s^{-1} wind speed, shown in Fig. 7, indicate that both angle-of-attack performance and zero pitch angle accuracy deteriorated as t/d increased beyond 0.037. The use of a deeper dimple can improve $\theta=0$ accuracy, but the poor angle of attack performance indicates that the use of significantly thick (i.e., $t/d>0.037$) probes is not recommended.

In an attempt to find a more easily machined substitute for the spherical arc-shaped dimple, a shallow conical dimple was tried on a $t/d=0.037$ probe. The center depth δ and dimple surface radius r were the same as that of the arc-shaped dimples used on the $t/d=0.037$ probe shown in Fig. 6. Wind tunnel tests presented in Fig. 8 show that at large s/d spacing ratios the conical dimple probe performed nearly as well as the equivalent spherical dimple probe. However, at small s/d spacings the angle-of-attack response of the conical dimple probe was much poorer than that of the equivalent $t/d=0.037$ spherical dimple probe. In general, the use of a conical dimple gave a somewhat poorer overall combination of $\theta=0$ accuracy and angle-of-attack performance. However its ease of machining warrants its continued consideration, especially if exacting accuracy is not needed.

c. Response to wind speed changes, $U_\infty=10$, 15, 20 m s^{-1}

The flat $t/d=0.011$ reference probe and the arc dimple $t/d=0.037$ probe were tested at wind speeds of 10, 15, and 20 m s^{-1}. The results were tabulated as a function of spacing ratio and wind speed. Presented in Table 2 are the useful $\pm\theta$ angle of attack range, the mean error over the specified $\pm\theta$ range, and the useful range of turbulence intensity for each probe. Useful angles of attack were defined as the angle-of-attack range over which the standard deviation of the pressure error about the mean did not exceed 0.5%. Useful angle-of-attack ranges based on $\pm 0.5\%$ deviation from the $\theta=0$ mean error were typically ± 2 to $\pm 3°$ less than the values given in Table 2. The role of turbulent

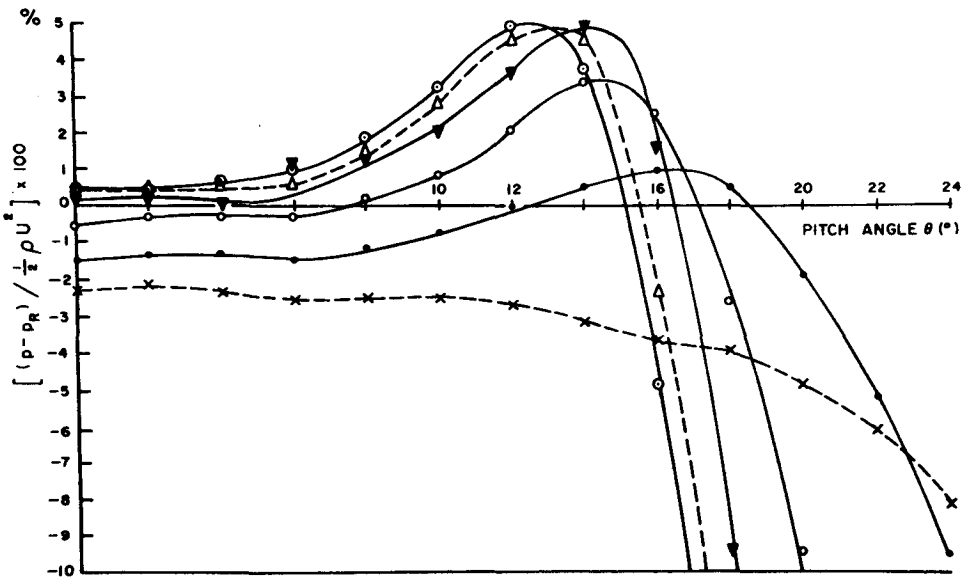

FIG. 8. Details of static pressure error characteristics of a $t/d=0.037$ probe (with conical shaped dimples) versus plate spacing and pitch angle for $U_\infty \approx 10$ m s^{-1}: ⊙, $s/d=0.8$; △, $s/d=0.7$; ▼, $s/d=0.6$; $s/d=0.5$; ●, $s/d=0.4$; ×, $s/d=0.3$.

TABLE 2. Double disk static head sensor, useful angle-of-attack ranges and accuracies.

Probe: $t/d=0.011$, comparison probe, no dimple

Spacing ratio s/d	$U_\infty=10$ m s^{-1} $\pm\theta$	$\bar{C}(\pm\theta)$ (%)	u' (rms) (%)	$U_\infty=15$ m s^{-1} $\pm\theta$	$\bar{C}(\pm\theta)$ (%)	u' (rms) (%)	$U_\infty=20$ m s^{-1} $\pm\theta$	$\bar{C}(\pm\theta)$ (%)	u' (rms) (%)
0.40	±16°	−1.9	14	±16°	−1.9	14	±16°	−1.8	14
0.47	±13°	−1.1	11	±13°	−1.1	11	±12°	−0.9	10
0.50	±12°	−0.9	10	±12°	−1.0	10	±12°	−0.9	10
0.57	±10°	−0.9	9	±10°	−1.1	9	±10°	−1.0	9
0.60	±10°	−0.8	9	±10°	−1.0	9	±9°	−1.0	8
0.70	±9°	−0.3	8	±9°	−0.5	8	±8°	−0.6	7

Probe: $t/d=0.037$, test probe, arc dimple

Spacing ratio s/d	$U_\infty=10$ m s^{-1} $\pm\theta$	$\bar{C}(\pm\theta)$ (%)	u' (rms) (%)	$U_\infty=15$ m s^{-1} $\pm\theta$	$\bar{C}(\pm\theta)$ (%)	u' (rms) (%)	$U_\infty=20$ m s^{-1} $\pm\theta$	$\bar{C}(\pm\theta)$ (%)	u' (rms) (%)
0.3	±15°	−1.4	13	±15°	−1.4	13	±14°	−1.7	12
0.4	±15°	−0.2	13	±15°	+0	13	±15°	+0.1	13
0.5	±12°	+0.5	10	±12°	+1.0	10	±12°	+0.7	10
0.6	±10°	+0.9	9	±11°	+0.8	9.6	±11°	+0.7	9.6
0.7	±10°	+1.4	9	±10°	+1.2	9	±10°	+1.3	9
0.8	± 9°	+1.5	8	±10°	+1.4	9	±10°	+1.2	9

Probe: $t/d=0.005$, Robertson (1972), no dimple

Spacing ratio s/d	$U_\infty \approx 7$ m s^{-1} $\pm\theta$	$\bar{C}(\pm\theta)$ (%)	u' (rms) (%)
0.40	±16°	−1.4	14
0.50	±11°	−0.8	10
0.67	±8°	−0.6	7

intensities will be discussed shortly. In general, the results show that although actual unnormalized static pressure errors increased with increasing wind speed, the average angle-of-attack error when normalized with the increasing dynamic pressure head did not change significantly. Robertson's results for a $t/d=0.005$ probe with no dimples are also shown in Table 2 for comparison. It is not clear what criteria Robertson used to determine his $\pm\theta$ values, but his results are in general agreement with ours.

The probe tests reported here were conducted in a low turbulence wind field. However, some estimates of the influence of turbulent gusts on the performance of the probe were obtained by treating changes in angle of attack as due to the addition of turbulent velocity components to a mean wind parallel to the probe, Robertson (1972). The results are summarized in Table 2 for the flat $t/d=0.011$ and the arc dimple $t/d=0.037$ probes. Robertson's (1972) results are also given.

d. Errors due to mounting supports and plate spacing rods

The plate spacing rods in the 0.037 probe were roughly 30 rod diameters ahead of the sensing ports. The influence of these spacing rods on the sensitivity of the probes to horizontal variations in wind direction was tested by rotating the probe so that a spacing rod faced directly into the prevailing wind and hence was in front of the sensing ports. No significant increase in measured static pressure errors was observed when this was done. Apparently, the rods were sufficiently ahead of the ports so that shed vortices had time to damp out. Similarly the spacing rods were not found to influence angle of attack performance. Vortex shedding frequencies of the rods based on the Kármán shedding relation are much higher than any response time characteristics of our probes.

The geometry of the probe support (used to attach the lower disk to a mounting rod) did exert a significant influence on the symmetry of the probe's angle of attack performance, however. As can be seen in Fig. 3, some asymmetry in the error curves was found as θ went from (+) to (−) angles. This was attributed to a probe mount blocking influence, since, when the probe orientation was reversed in the tunnel, the asymmetry of the curves reversed. The probe mount support influence was greatest when the probe was tilted so that the mounting stem faced the incoming airstream (i.e., the opposite wind attack angle shown in Fig. 1). Apparently, the base mounting caused flow along the bottom disk to differ somewhat from that along the upper disk. This introduced an asymmetry in the $\pm\theta$ angle-of-attack response of the probes which varied according to the geometry and projected area of the base support. When the support was reduced to as small a size as possible, the angle-of-attack asymmetry became accordingly less pronounced. The most suitable mounting arrangement was found to be a simple cylindrical rod, flush mounted against the lower disk, with no flaring or contouring connection.

One last point should be noted, and that was the need to maintain parallel alignment of the two disks once a spacing ratio had been chosen. Misaligned plates introduced erratic errors into the probe's angle of attack response, as well as to the probe's accuracy at $\theta=0$. No systematic check of misalignment induced errors was attempted. However, considerable care was taken to insure that the two disks were properly aligned during testing.

5. Discussion of probe performance

A qualitative explanation of the error compensating nature of the double disk design can be partially provided by the tendency of a flat plate in an air stream to act like an air foil (i.e., have a finite circulation) and experience lift due to pressure differences across the plate (Fig. 9). Thus, in the simplest analysis, the port in the upper plate in Fig. 1 should read a slightly higher pressure than the opposite facing port in the lower plate. When averaged together in a balancing chamber, some pressure error balancing will occur.

Besides the compensating nature of mutually facing ports, the double-disk design seems to have one other primary advantage, namely, an apparent tendency to inhibit leading edge air flow separation and the formation of so-called separation bubbles over the plate surface and ports. This can best be described in terms of a channeling or ducting effect which tends to make to flow between the plates more parallel to the inner plate surfaces. To picture this effect, visualize the composite flow pattern that would result from two plates, each with flow patterns similar to that shown in Fig. 9 when placed one over the other.

It has been suggested (personal communication, R. A. Panton) that the pressure curve skirts [i.e., rises at roughly $\theta\approx\pm16°$ in the pressure error diagram (Fig. 3) for example] may be associated with separation effects. Note that the curves for small spacing are flatter, and the skirts occur at larger $\pm\theta$, as the spacing ratio s/d decreases to near 0.4. This behavior qualitatively agrees with a channeling effect.

The influence of the dimples via Bernonlli's relation

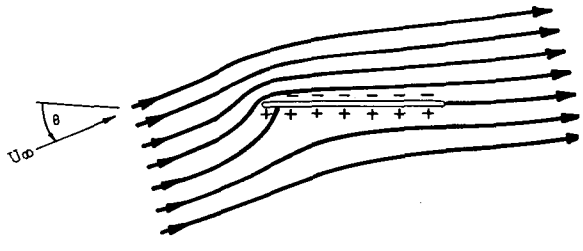

FIG. 9. Flow pattern around an inclined plate in a uniform air stream at angle of attack θ. (+) and (−) symbols indicate excesses and deficits of pressure (relative to ambient) due to finite circulation (Prandtl and Tietjens 1954).

has already been referred to in our design procedure. Accelerations due to curvature, and consequent distortion of streamline spacing (see Fig. 2) are compensated for by using dimples to decelerate the flow and return the local pressure to its ambient static value. The influence of the dimples at non-zero attack angles is not well understood but should be aided by the channeling effect of the double-disk arrangement.

6. Conclusions

The results of our tests show that air flow curvature induced static pressure errors can be minimized by the use of compensating dimples. The circular symmetry of our probes eliminates yaw errors. Useful angle-of-attack range is a maximum somewhere between $0.3<s/d<0.4$, and decreases as s/d increases. In contrast $\theta=0$ accuracy for a given dimple geometry (or no dimple) improves as s/d increases. The best overall performance was obtained with the $t/d=0.011$ flat surface probe. If one's application can tolerate external tubing then this probe is recommended. If a more rugged probe with a self-contained internal tubing arrangement is desried, and a slight reduction in error performance can be tolerated, then the $t/d=0.037$ dimpled probe is recommended. The ad hoc design procedure outlined earlier seems to provide reasonable starting values for dimple design. Test results indicate that because of the mutual influence of each disk on the flow over the other, a slightly deeper dimple should be used than indicated by our simple theory. Trial and testing indicated that dimple depth in a double-disk design should be increased by at least 25–30% over that indicated by the design procedure for a single disk.

Acknowledgments. The author would like to thank Professor E. Kraus for his support, and Dr. J. Sparkman and the National Oceanographic and Atmospheric Administration for the use of the Mississippi Test Facility wind tunnel. This work was partially supported by the National Science Foundation under Grant GA 33550X.

REFERENCES

Bryer, D. W., and R. C. Pankhurst, 1971: Pressure-probe methods for determining wind speed and direction. London, H. M. Stationary Office.

Elliot, J. A., 1972: Instrumentation for measuring static pressure fluctuations with the atmospheric boundary layer. *Bound-Layer Meteor.*, **2**, 476.

Franklin, R. E., and J. M. Wallace, 1970: Absolute measurements of static-hole error using flush transducers. *J. Fluid Mech.*, **42**, Part 1, 33–48.

Hasselmann, K., *et al.*, 1973: Measurement of wind-wave growth and swell decay during the Joint North Sea Wave Project (JONSWAP). *Deut. Hydrogr. Z.*, **A12**, Suppl. 95 pp.

Milne-Thomson, L. M., 1960: *Theoretical Hydrodynamics*, 4th ed. MacMillan Co., 743 pp.

Prandtl, L., and O. G. Tietjens, 1954: *Applied Hydro- and Aeromechanics*. Dover, 306 pp.

Robertson, P., 1972: A direction-insensitive static head sensor. *Sci. Instrum.*, **5**, 1080–1082.

Thompson, N., 1975: *Royal Society Air-Sea Interaction Project*. The Royal Society, London, 98.